William Cain, Allison E. Fetz, Gary L. Bowlin

Evaluating the Effect of Incorporation of Fibrinogen into Electrospun Templates of Polydioxanone on their Mechanical Properties

Faculty Sponsor

Dr. Gary Bowlin

Abstract

Research has shown that the enzyme matrix metalloproteinase-9 (MMP9) is a critical factor responsible for angiogenesis. Since MMP9 secretion by neutrophils can be induced by fibrinogen, our goal is to stimulate the secretion of MMP9 from template interacting neutrophils via the incorporation of fibrinogen into an electrospun template. The aims of this preliminary research study were (1) to create electrospun templates of five different concentrations of the synthetic polymer, polydioxanone, and the natural polymer, fibrinogen, (2) to analyze the fiber diameters of these templates, and (3) to characterize the mechanical properties of these templates. The results indicate that increased fibrinogen incorporation into polydioxanone templates correlates with a decrease in the fiber diameter of their resultant electrospun templates. Additionally, uniaxial tensile testing revealed that increasing the fibrinogen content of electrospun templates decreased both the ultimate tensile strength and the maximum strain of the electrospun template. This work shows that incorporation of fibrinogen into electrospun polydioxanone templates changes the mechanical properties of the templates, and thus alters the potential of the biomaterial to be used in applications which are subject to different stresses and strains. Future work will evaluate the effect that fibrinogen concentration makes on neutrophil secretion of MMP9 and its efficacy in inducing angiogenesis.

Introduction

Various pathologies are characterized by a lack of functional vascularization. One of the most prevalent conditions is peripheral arterial disease (PAD), which presents with atherosclerotic narrowing of the arteries of the limbs, especially the legs. PAD leads to pain and movement disabilities, secondary to muscle atrophy and non-healing ulcers. If the condition is left untreated, injury or ulcers in the ischemic tissue may lead to tissue death and gangrene and necessitate total limb amputation [1]. Treatment strategies include bypass surgery to restore blood flow to the ischemic tissues using allografts, autografts, and synthetic grafts. Since there is typically poor neointimal regeneration of these vascular grafts, thrombosis can occur, occlude the vessel, and cause the graft to fail at high rates [2]. This high failure rate indicates the need for a better system which can guide blood flow to targeted tissues. Ideally, a resorbable small diameter vascular graft could guide the in situ regeneration of a functional native blood vessel. To generate this functional graft, the template must guide robust angiogenesis by recruiting endothelial cells into the lumen of the graft and supporting their proliferation. This neointimal regeneration is essential for the success of the implant so that a confluent endothelium, neointima, can form [3-5].

The white blood cells that lead the immune system in the inflammatory response, the neutrophils, release an enzyme, MMP9, which has been identified as a critical factor responsible for angiogenesis [6-8]. Because implanted vascular grafts immediately interact with large numbers of neutrophils upon implantation and ligation of a receptor which binds fibrinogen (FBG) is known to induce neutrophil secretion of MMP9, we anticipate that we may be able to harness the angiogenic capabilities of neutrophils by incorporating FBG into electrospun templates of polydioxanone (PDO). Achievement of this aim will create more efficacious grafts for restoring blood flow to ischemic tissues.

To create these templates, we electrospun solutions containing different concentrations of PDO and FBG. Electrospinning is a process by which templates composed of nano- to microfibers are fabricated. This template fabrication process involves the application of a voltage source to a polymer solution which is stored in a syringe. Due to the potential difference between the liquid surface at the tip of the syringe and a grounded target opposite the syringe, a liquid jet extrudes from the syringe and is drawn across an airgap to deposit small diameter fibers onto the grounded target. This process creates mats of nonwoven, randomly distributed fibers, which are biomimetic of native extracellular matrix (ECM). These templates can be fabricated with an array of physical, chemical, and mechanical properties which create

efficacious biomaterials for diverse application in guided tissue regeneration.

Since FBG plays a key role in the secretion of MMP9 from neutrophils, we sought to incorporate this protein into our electrospun templates and determine if the physical and mechanical properties of these FBG containing templates differed significantly depending on their concentration ratio of PDO and FBG. The morphological characteristics of the templates were evaluated by fiber diameter analysis, which indicated that increasing the percentage of FBG in the templates decreases the average fiber size. The mechanical properties were evaluated by uniaxial tensile testing to determine Young's modulus (YM), Ultimate Tensile Strength (UTS), and maximum strain for each template. The data indicate an inverse correlation between the percentage of FBG and both UTS and maximum strain. Additionally, mechanical testing data displayed a non-uniform correlation between FBG concentration and YM, which indicated that some intermediate percentage of FBG incorporation may maximize the stiffness of the material. These results indicate that FBG incorporation into electrospun templates of PDO changes the properties of the templates, and, with these tailorable templates, we should be able to fabricate and optimize the FBG incorporation into templates to promote optimal MMP9 secretion.

Null Hypothesis

Incorporating FBG into electrospun PDO templates will not affect the mechanical properties of YM, UTS, or maximum strain.

Materials And Methods

Electrospinning

In this study, PDO (Bezwada Biomedical LLC, Lot. No. BB0306-234D) and FBG (Sigma, Fibrinogen from bovine plasma, F8630-5G, Lot. No. SLBW1275) were combined in different volume-to-volume ratios (vol/vol) to create templates with variable compositions of FBG (Table 1). The two polymers were dissolved in solution in separate vials. The PDO was mixed for 24 hours in a vial of 1,1,1,3,3,3-hexafluoro-2-propanol (HFP, Oakwood Products, Inc., Pro. No. 003409), and the FBG was mixed in a solution of 1 part 10x Gibco Minimum Essential Medium with Earle Salts (MEM, ThermoFisher Scientific, Cat. No. 11430030) to 9 parts HFP for 24 hours [9]. The PDO solution was added to the FBG vial after 24 hours, vortexed for 60 seconds, and then loaded into a 3-mL syringe (Becton, Dickinson, and Company, Pro. No. 309657). This syringe was attached to an 18-gauge blunt needle McMaster-Carr, Pro. No. 6710A25) which

was connected to the positive lead of a Spellman CZE1000R power source (Spellman High Voltage Electronic Corp.). The syringe was placed on a syringe pump (Fisher Scientific, Model No. 78-01001) which dispensed the solution at a rate between 0.25 mL/h and 2.00 mL/h. Fibers were collected on the parchment side of non-stick Pan Lining Paper (Reynolds Wrap, Model No. B0068TZUXO) which was attached to a grounded, stainless steel 200 x 750 x 5 mm rectangular mandrel, which was rotating at 1250 RPM and translating 6.5 cm/s over 13 cm. Polymer concentration, applied voltage, flow rate, and airgap distance between the needle tip and mandrel are shown in Table 1. The parameters were optimized for each electrospun template to produce templates composed of uniform fiber diameter which were non-beaded. The templates (thickness 0.07 - 0.13 mm) were stored in a desiccator at 25°C until analysis connected to the positive lead of

PDO/FBG (vol/vol)	PDO Concentration (mg/mL)	FBG Concentration (mg/mL)	Voltage (kV)	Flow Rate (mL/h)	Airgap Distance (cm)
100/0	67	N/A	+14	0.25	14
75/25	60	100	+28	2.00	15
50/50	100	100	+28	2.00	15
25/75	100	100	+28	2.00	15
0/100	N/A	100	+28	2.00	15

Table 1. Electrospinning parameters optimized for PDO/FBG templates.

a Spellman CZE1000R power source (Spellman High Voltage Electronic Corp.). The syringe was placed on a syringe pump (Fisher Scientific, Model No. 78-01001) which dispensed the solution at a rate between 0.25 mL/h and 2.00 mL/h. Fibers were collected on the parchment side of non-stick Pan Lining Paper (Reynolds Wrap, Model No. B0068TZUXO) which was attached to a grounded, stainless steel 200 x 750 x 5 mm rectangular mandrel, which was rotating at 1250 RPM and translating 6.5 cm/s over 13 cm. Polymer concentration, applied voltage, flow rate, and airgap distance between the needle tip and mandrel are shown in Table 1. The parameters were optimized for each electrospun template to produce templates composed of uniform fiber diameter which were non-beaded. The templates (thickness 0.07 - 0.13 mm) were stored in a desiccator at 25°C until analysis.

Imaging and Fiber Diameter Analysis

To characterize the templates by scanning electron microscopy, each template was sputter coated with 5 nm of gold-palladium in an argon gas field. The templates were then imaged using a scanning electron microscope (SEM, FEI Nova NanoSEMTM 650) with a field emission gun at + 20 kV and a working distance of 5 mm. Both the inside (mandrel facing) and outside (external facing) surfaces of each template were imaged at 1000x and 5000x to ensure the templates were composed of non-fused, non-beaded fibers. If the SEM image revealed a template composed of beaded or fused fibers, the template was discarded, and the fabrication and characterization process was repeated until optimal electrospinning parameters were found. The fiber diameters were subsequently quantified by analyzing the SEMs in FibraQuant 1.3 software (nanoTemplate Technologies, LLC). A minimum of 200 semi-automated random measurements were taken per image to generate averages and corresponding standard deviations.

Mechanical Testing

After fabrication and SEM characterization, the electrospun templates were cut into dogbone shaped samples (2.75 mm at the narrowest point) in two directions: axial (parallel to the axis of rotation) and perpendicular (perpendicular to the axis of rotation). The thickness of each specimen was measured using calipers (Mitutoyo Absolute, Pro. No. 547-516), and the dogbone shape samples were loaded into a TestResources frame (model no. 220Q with 111 N load cell) with a gauge length of 7.5 mm. Uniaxial tensile testing was then performed ($n \geq 7$ punches of each orientation) at a strain rate of 10 mm/min until failure. The resultant data were recorded in the software associated with the testing frame (TestResources XY Series Software) and exported to Microsoft Excel.

Data and Statistical Analysis

Microsoft Excel was used to generate stress strain curves for each replicate, which was then used to calculate YM, UTS, and maximum strain. YM for each template was found using a line of best fit to approximate the slope of the initial linear elastic region of the stress strain curve. The slope of each linear elastic region, equivalent to the YM of that piece of electrospun material, was recorded and saved for statistical analysis. Similarly, the UTS was identified by finding the maximum stress on the stress strain curve. This peak stress occurs just before the material fails under uniaxial tensile testing. Last, the maximum strain was found and corresponds to elongation at the point of failure. The data were grouped by the orientation of the dogbone punch and exported to Graphpad Prism 6 for statistical analysis.

The normality of the data was tested using the Shapiro-Wilk normality test to determine the appropriate analysis of variance. Fiber diameter and each mechanical property was then analyzed with either Kruskal-Wallis analysis of variance and Dunn's multiple comparison procedure for non-normal data sets or Tukey's multiple comparisons test for normal data. All analyses were performed in GraphPad Prism 6 at a significance level of 0.05.

Results

Electrospinning and Fiber Diameter Analysis

The electrospinning parameters for each PDO/FBG mixture were optimized to produce fibers which were approximately equivalent to those of the lowest concentration of PDO. After these parameters were optimized such that the electrospun fibers were non-fused, non-beaded, and roughly the same diameter, full templates of each composition were fabricated. Figure 1 shows representative SEMs which display the fiber morphology of each template. As shown in Figure 1, there appears to be some inconsistency in the fiber deposition patterns between the five templates including relative alignment of the fibers and presence of both large and small fibers in some templates (Figure 1D). Worthy of note, the PDO/FBG template 0/100 (Figure1E) has a single fiber which has an elongated bead and appears to have fibers packed in greater density than the other templates. As fiber anisotropy and density of the templates were outside of the scope of this project, we did not further investigate these properties.

The results of fiber diameter analysis are shown in Figure 2 and Table 2. As indicated in Figure 2, the average fiber diameter of the templates correlates inversely to the percentage of FBG incorporated into the electrospun templates. The average fiber diameter of each PDO containing electrospun template decreased with increasing proportions of FBG incorporation. Notably, the 0.28 ± 0.14 μm fibers for the PDO/FBG 100/0 template were significantly larger ($p < 0.05$) than all other templates while the 0.17 ± 0.09 μm fibers for the PDO/FBG 25/75 template were significantly smaller ($p < 0.05$) than for all other templates. The PDO/FBG 0/100 electrospun template did not continue the same trends as the blended templates which contained PDO.

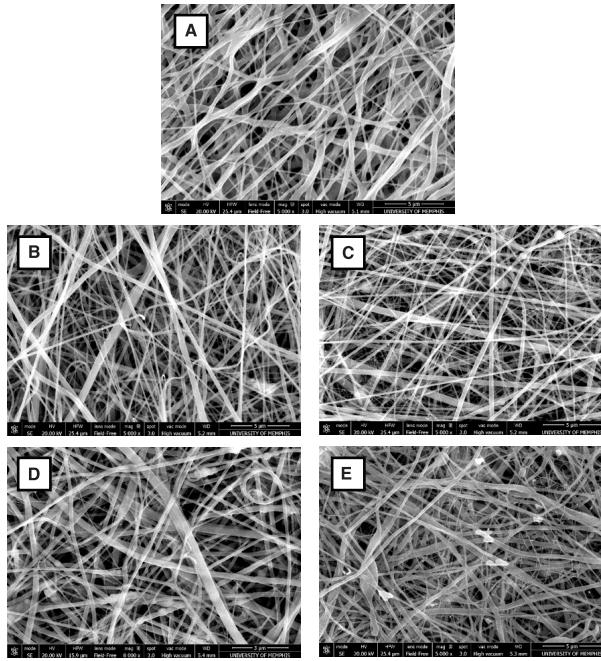

Figure 1. Electrospun templates of PDO/FBG vol/vol A)100/0, B) 75/25, C) 50/50, D) 25/75, and E) 0/100 (images taken at 5000x (A, B, C, E) and 8000x (D), scale bars = 5 μm (A, B, C, E) and 3 μm (D)).

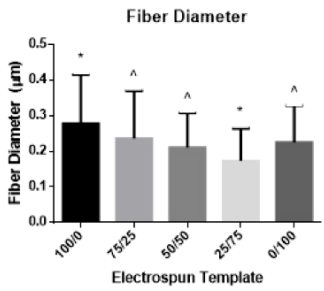

Figure 2. Fiber diameter for each electrospun template. *indicates significant difference from all other templates. ^ indicates significant difference from 100/0 and 25/75 ($p < 0.05$).

PDO/FBG (vol/vol)	Fiber Diameter (μM)
100/0	0.28 ± 0.14
75/25	0.24 ± 0.13
50/50	0.21 ± 0.10
25/75	0.17 ± 0.09
0/100	0.23 ± 0.10

Table 2. Mean and standard deviation for fiber diameter.

Mechanical Testing

Results for the mechanical testing are shown in tabular format in Table 3. Results are reported as mean ± standard deviation for at least 7 replicates. Units for YM and UTS are megapascals (MPa) and units for maximum strain are strain (ε) which is a unitless measurement for distance/distance.

PDO/FBG (vol/vol)	YM (MPA)		UTS (MPA)		Maximum Strain (ε)	
	Axial	Perpendicular	Axial	Perpendicular	Axial	Perpendicular
100/0	33 ± 4	26 ± 10	7.8 ± 0.8	10.0 ± 2.0	0.65 ± 0.14	0.50 ± 0.05
75/25	85 ± 43	70 ± 30	9.6 ± 1.9	8.6 ± 2.2	0.27 ± 0.07	0.27 ± 0.09
50/50	57 ± 22	22 ± 7	5.7 ± 0.9	4.1 ± 0.6	0.19 ± 0.03	0.25 ± 0.02
25/75	72 ± 27	66 ± 23	3.8 ± 0.5	3.2 ± 0.4	0.12 ± 0.01	0.12 ± 0.06
0/100	35 ± 9	27 ± 12	1.0 ± 0.3	1.0 ± 0.3	0.08 ± 0.01	0.09 ± 0.02

Table 3. Mean and standard deviation for YM, UTS, and maximum strain.

Figure 3 shows the results for YM and indicate variability in stiffness of the templates. Mechanical testing data shown in Figure 3 revealed larger average YM for PDO/FBG 75/25 and 25/75 templates than for PDO/FBG 100/0, 50/50, and 0/100 templates. These trends were significant for the perpendicular orientation (i.e. 75/25 and 25/75 template YM were significantly greater than all other templates of that orientation). For axial orientation data, the same peaks and troughs were indicated; however, there was no significant difference for the PDO/FBG 50/50 template.

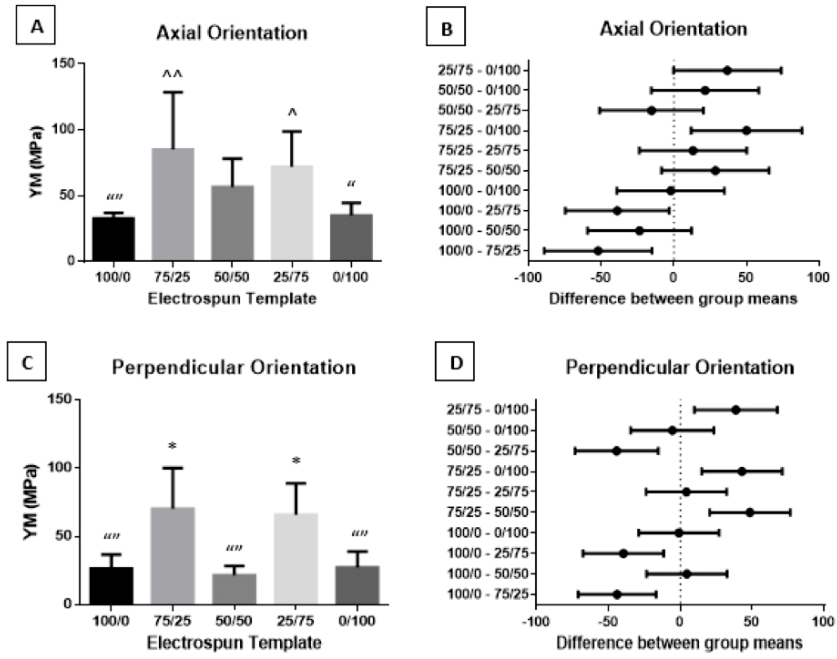

Figure 3. YM histograms with 95% confidence intervals (Tukey's) for (A and C) axial and (B and D) perpendicular oriented punches. “” indicates significant difference from 75/25 and 25/75. ^^ indicates significant difference from 100/0 and 0/100. ^ indicates significant difference from 100/0. “ indicates significant difference from 75/25. * indicates significant difference from all other templates ($p < 0.05$).

Figure 4 shows the histograms and 95% confidence intervals for the UTS of the PDO and FBG templates. The data suggest that UTS decreases with increasing FBG percentage for all electrospun templates, excluding PDO/FBG 100/0 when axially tested. Excluding the aforementioned template, the UTS for axial punches significantly decreased with increasing FBG incorporation. The perpendicular results showed that PDO/FBG templates with greater than 50% PDO were significantly stronger than all other templates.

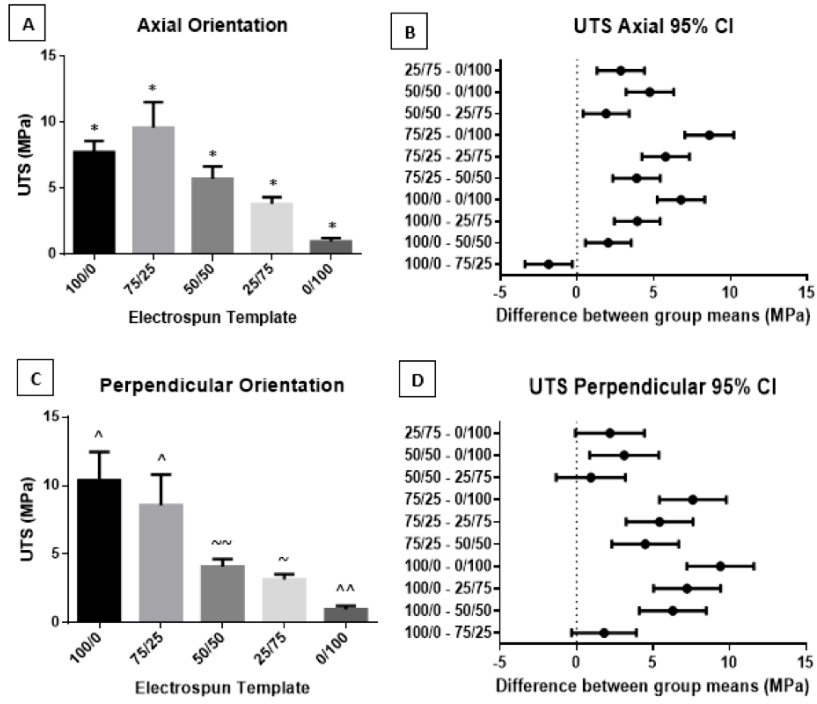

Figure 4. UTS histograms with 95% confidence intervals (Tukey's) for (A and C) axial and (B and D) perpendicular oriented punches. * indicates significant differences from all other templates. ^ indicates significant differences from 50/50, 25/75, and 0/100. ~~ indicates significant differences from 100/0, 75/25, and 0/100. ~ indicates significant differences from 100/0 and 75/25. ^^ indicates significant differences from 100/0, 75/25, and 50/50 ($p < 0.05$).

Figure 5 shows the histograms and 95% confidence intervals for the maximum strain of the PDO and FBG templates. The data shown in Figure 5 followed the general trend of decreasing maximum strain with increasing FBG incorporation. For the axial orientation templates, statistically significant differences were found in each comparison except 25/75 vs. 0/100, 50/50 vs. 25/75, and 75/25 vs. 50/50. Similarly, for the perpendicular orientation punches statistically significant differences were demonstrated in each comparison except 25/75 vs. 0/100 and 75/25 vs. 50/50.

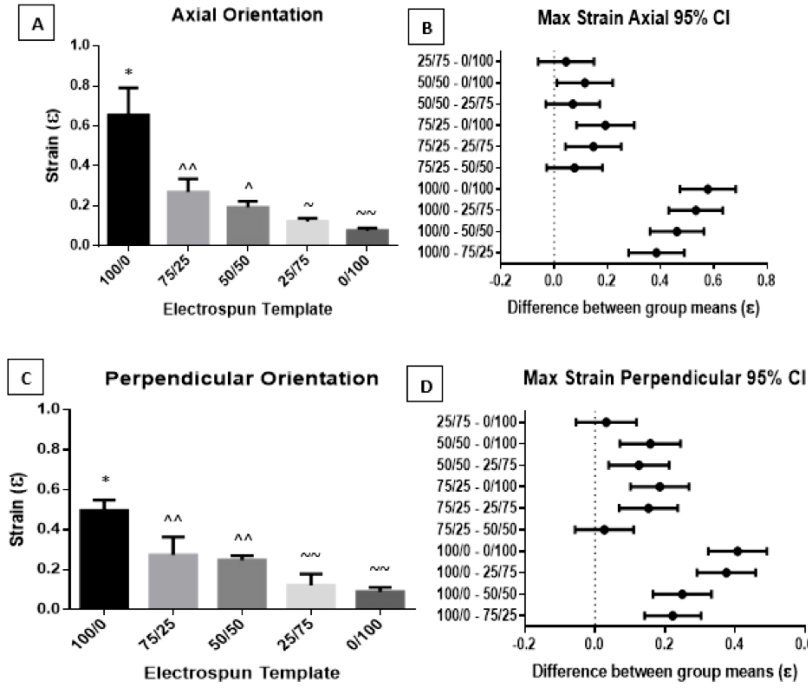

Figure 5. Maximum strain histograms with 95% confidence intervals (Tukey's) for (A and C) axial and (B and D) perpendicular oriented punches. * indicates a significant difference from all other templates. ^^ indicates a significant difference from 100/0, 25/75, and 0/100. ^ indicates a significant difference from 100/0 and 0/100. ~ indicates a significant difference from 100/0 and 75/25. ~~ indicates a significant difference from 100/0, 75/25, and 50/50 ($p < 0.05$).

Discussion

Conditions characterized by a lack of functional vascularization, such as PAD, may have blood flow restored to ischemic tissues via controlling the angiogenic abilities of MMP9 secretion from neutrophils. Since FBG has been shown to regulate the secretion of MMP9, we sought to incorporate this polymer into electrospun templates and stimulate the secretion of MMP9, thus inducing angiogenesis. Initially, our goal for the project was to fabricate electrospun templates for each vol/vol ratio of PDO and FBG with two different sizes of fibers in order to explore fiber diameter as another independent variable. After multiple repetitions of varying the concentration of PDO, the concentration of FBG, and the electrospinning parameters of the different solutions and still producing substandard templates (i.e. single solutions which yielded electrospun fibers of two extremely different diameters or templates which were composed of heavily beaded fibers), we focused on the successful fabrication of just one template per vol/vol ratio and evaluating the mechanical properties of these templates in comparison to one another.

The fiber diameter of the templates was a primary focus in the fabrication of these PDO/FBG templates. The PDO/FBG 100/0 template was electrospun at the lowest concentration possible with parameters refined to generate the smallest fibers possible from the Bezwada PDO. The smallest amount of FBG incorporation, just 25% by volume in PDO/FBG 75/25, yielded fibers which were smaller than those possible with electrospun PDO. Increasing FBG incorporation decreased the size of the fibers further until the PDO/FBG 0/100 template was fabricated. Electrospinning of this exclusively FBG solution produced fibers which were larger than those of both template 75/25 and template 50/50. This indicates that the mere combination of PDO and FBG may decrease the fiber size of their resultant electrospun templates. This change in template properties may be due to polymer chain entanglement in solution during the process of electrospinning or the degree of crystallinity of templates which contain both polymers.

Like the fiber size of the templates, the mechanical properties of each template varied with different degrees of FBG incorporation. The results for YM indicate that the stiffness of the electrospun material is influenced by percentage of FBG. YM was the greatest in the PDO/FBG 75/25 and 25/75 templates. This indicates an increase in rigidity when some intermediate amount of FBG is incorporated into a template between 0% and 50% and between 50% and 100%. Since no statistically significant difference was found in YM when comparing PDO/FBG templates of 100/0, 50/50, or 0/100, there is insufficient evidence to conclude that a combination of the polymers alone

increases the YM of electrospun PDO and FBG.

Trends in the data for both UTS and maximum strain indicate that mechanical strength decreases with increasing amounts of FBG in electrospun templates. With the exception of the axial PDO/FBG 100/0, all average values for UTS and strain decreased with an increase in percentage of FBG incorporation in the electrospun templates. Whereas this does indicate that electrospun PDO templates are more robust and durable with less FBG incorporation, it does not mean the templates composed of primarily FBG are inferior candidates for tissue regeneration. The UTS of the ECM of some tissues *in vivo*, such as the aorta, is 1.02 MPa [10]. This UTS is almost equivalent to that of the PDO/FBG 0/100 template (0.99 ± 0.28 MPa) which was fabricated from exclusively FBG. Therefore, the diminished strength of the FBG incorporated electrospun templates may make it the optimal electrospun material for certain tissue regeneration applications.

The UTS and maximum strain trends were similar to the trends in fiber diameter and indicate that the reduced fiber diameters decrease UTS and maximum strain. However, the fiber diameter of the PDO/FBG 0/100 template was significantly larger than the fiber diameter of PDO/FBG 25/75 template, yet the PDO/FBG 0/100 had the lowest UTS and maximum strain. Despite this elevated fiber diameter, the average UTS and maximum strain stayed consistent in their trends and reached their lowest point at PDO/FBG 0/100. This suggests that the decreases in UTS and maximum strain are due to percentage FBG incorporation instead of decreases in fiber diameter.

A potential concern regarding electrospun FBG is fiber diameter and the induced immune response. Our research has shown that high surface area to volume ratio increases the neutrophil response of NETosis on implanted PDO templates [12]. Since increasing the fiber diameter of electrospun FBG incorporated templates has heretofore been unsuccessful, an abundant inflammatory response may be problematic when neutrophils interact with FBG incorporated templates if we cannot electrospin larger diameter templates. However, since FBG is a natural polymer, it may inherently provoke less of an inflammatory response when electrospun than PDO even on high surface area to volume ratio templates. Therefore, the scaling down of the fiber diameter may be unnecessary for the successful fabrication of FBG incorporated electrospun templates.

If the templates are durable enough to be implanted without mechanical failure, can effectively facilitate angiogenesis, and do not significantly change in mechanical strength when hydrated, the templates may be suitable tissue regeneration templates for the treatment of PAD. Since each template was able to be handled through the cutting and testing process and demonstrated

mechanical characteristics greater than or equal to those of some decellularized ECM, the FBG incorporated templates should progress to the next stage of testing [11]. Future work on this project includes further electrospinning to fabricate FBG incorporated templates of larger fiber diameter and in vitro testing of these templates to verify and substantiate the claim that electrospun FBG upregulates the release of MMP9 from interacting neutrophils. Eventual research will test for the efficacy of this biomaterial in inducing robust angiogenesis.

Conclusion

This project has initiated the investigation into the effect that FBG incorporation has on electrospun PDO templates. Our research sought to create electrospun templates of five different concentrations of PDO and FBG and analyze the properties of each template. The project has given us sufficient evidence to refute our null-hypothesis and conclude that the incorporation of FBG into electrospun PDO templates does affect the mechanical properties of YM, UTS, and maximum strain. Increased FBG decreases the size of electrospun fibers and may decrease the possible range of fiber diameters which can be electrospun. Additionally, FBG incorporation influences YM of fabricated templates, and, in general, increasing the percentage of FBG in the electrospinning solution decreases the UTS and maximum strain of the template. This work holds significance in the field of guided tissue regeneration by demonstrating that different physical and mechanical properties of electrospun PDO may be tailored by the incorporation FBG. Future work will help in the determination if electrospun FBG will upregulate the secretion of MMP9 from neutrophils and spur angiogenesis, thereby increasing the efficacy of treatments for conditions such as PAD.

Acknowledgements

First, I would like to thank Dr. Bowlin for giving me the chance to work in his lab. He has been an outstanding mentor for me and has given me so many opportunities to excel in research over the last four years. I would also like to thank Allison Fetz for her continued assistance and patience with me as I learn new skills inside and outside of the lab. Additional thanks go out to each of my lab colleagues who have helped me with various issues associated with my research over the duration of this project and who have made the lab environment fun to work in. Research reported in this publication was supported by the National Institute of Biomedical Imaging and Bioengineering of the National Institutes of Health under Award Number R21EB024131 (GB). The content is solely the responsibility of the authors and does not necessarily represent the official views of the National Institutes of Health.

References

[1] Y. Ostchega, R. Paulose-Ram, C.F. Dillon, Q. Gu, J.P. Hughes. Prevalence of Peripheral Arterial Disease and Risk Factors in Persons Aged 60 and Older: Data from the National Health and Nutrition Examination Survey 1999–2004, *Journal of the American Geriatrics Society 55*(4) (2007) 583-589.

[2] M.J. Collins, X. Li, W. Lv, C. Yang, C.D. Protack, A. Muto, C.C. Jadlowiec, C. Shu, A. Dardik. Therapeutic Strategies to Combat Neointimal Hyperplasia in Vascular Grafts, *Expert Review of Cardiovascular Therapy 10*(5) (2012) 635-647.

[3] M. Hong-De Wu, Q. Shi, Y. Onuki, Y. Kouchi, L.R. Sauvage. Histologic Observation of Continuity of Transmural Microvessels Between the Perigraft Vessels and Flow Surface Microostia in a Porous Vascular Prosthesis, *Annals of Vascular Surgery 10*(1) (1996) 11-15.

[4] T. Pennel, D. Bezuidenhout, J. Koehne, N.H. Davies, P. Zilla. Transmural Capillary Ingrowth is Essential for Confluent Vascular Graft Healing, *Acta Biomaterialia 65* (2018) 237-247.

[5] F.J. Schoen. Interventional and Surgical Cardiovascular Pathology: Clinical Correlations and Basic Principles, *WB Saunders Company* 1989.

[6] V.C. Ardi, T.A. Kupriyanova, E.I. Deryugina, J.P. Quigley. Human Neutrophils Uniquely Release TIMP-free MMP-9 to Provide a Potent Catalytic Stimulator of Angiogenesis, *Proceedings of the National Academy of Sciences 104*(51) (2007) 20262-20267.

[7] V.C. Ardi, P.E. Van den Steen, G. Opdenakker, B. Schweighofer, E.I. Deryugina, J.P. Quigley. Neutrophil MMP-9 Proenzyme, Unencumbered by TIMP-1, Undergoes Efficient Activation In Vivo and Catalytically Induces Angiogenesis via a Basic Fibroblast Growth Factor (FGF-2)/FGFR-2 Pathway, *Journal of Biological Chemistry 284*(38) (2009) 25854-25866.

[8] E.I. Deryugina, E. Zajac, A. Juncker-Jensen, T.A. Kupriyanova, L. Welter, J.P. Quigley. Tissue-infiltrating Neutrophils Constitute the Major In Vivo Source of Angiogenesis-inducing MMP-9 in the Tumor Microenvironment, *Neoplasia 16*(10) (2014) 771-788.

[9] Rodriguez, I. (2010). *Mineralization Potential of Electrospun PDOnHA- Fibrinogen Scaffolds Intended for Cleft Palate Repair* (dissertation).

[10] Muiznieks, L. D., & Keeley, F. W. (2013). Molecular assembly and mechanical properties of the extracellular matrix: A fibrous protein perspective. *Biochimica Et Biophysica Acta (BBA) - Molecular Basis of Disease, 1832*(7), 866–875.

[11] Beenakker, J.-W. M., Ashcroft, B. A., Lindeman, J. H., & Oosterkamp, T. H. (2012). Mechanical Properties of the Extracellular Matrix of the Aorta Studied by Enzymatic Treatments. *Biophysical Journal 102*(8), 1731–1737.

[12] Fetz, A. E., Neeli, I., Rodriguez, I. A., Radic, M. Z., & Bowlin, G. L. (2017). Electrospun Template Architecture and Composition Regulate Neutrophil NETosis In Vitro and In Vivo. *Tissue Engineering Part A 23*(19-20), 1054–1063.